J Mater Sci: Mater Med (2010) 21:1799–1809
DOI 10.1007/s10856-010-4047-z

The stability mechanisms of an injectable calcium phosphate ceramic suspension

Ahmed Fatimi · Jean-François Tassin · Monique A. V. Axelos · Pierre Weiss

Received: 18 November 2009 / Accepted: 1 March 2010 / Published online: 13 March 2010

Abstract Calcium phosphate ceramics are widely used as bone substitutes in dentistry and orthopedic applications. For minimally invasive surgery an injectable calcium phosphate ceramic suspension (ICPCS) was developed. It consists in a biopolymer (hydroxypropylmethylcellulose: HPMC) as matrix and bioactive calcium phosphate ceramics (biphasic calcium phosphate: BCP) as fillers. The stability of the suspension is essential to this generation of "ready to use" injectable biomaterial. But, during storage, the particles settle down. The engineering sciences have long been interested in models describing the settling (or sedimentation) of particles in viscous fluids. Our work is dedicated to the comprehension of the effect of the formulation on the stability of calcium phosphate suspension before and after steam sterilization. The rheological characterization revealed the macromolecular behavior of the suspending medium. The investigations of settling kinetics showed the influence of the BCP particle size and the HPMC concentration on the settling velocity and sediment compactness before and after sterilization. To decrease the sedimentation process, the granule size has to be smaller and the polymer concentration has to increase. A much lower sedimentation velocity, as compared to Stokes law, is observed and interpreted in terms of interactions between the polymer network in solution and the particles. This experimentation highlights the granules spacer property of hydrophilic macromolecules that is a key issue for interconnection control, one of the better ways to improve osteoconduction and bioactivity.

A. Fatimi · P. Weiss (✉)
Laboratoire d'Ingénierie Ostéo-Articulaire et Dentaire (LIOAD), INSERM U791, 1 place Alexis Ricordeau, BP 84215, 44042 Nantes Cedex 1, France
e-mail: pierre.weiss@univ-nantes.fr; pweiss@sante.univ-nantes.fr

A. Fatimi · P. Weiss
Laboratoire d'Ingénierie Ostéo-Articulaire et Dentaire (LIOAD), Université de Nantes, 1 place Alexis Ricordeau, 44042 Nantes Cedex 1, France

J.-F. Tassin
Laboratoire Polymères, Colloïdes, Interfaces (LPCI), UMR 6120, CNRS, Université du Maine, Avenue Olivier Messiaen, 72085 Le Mans Cedex 9, France

M. A. V. Axelos
INRA, UR1268 Biopolymères Interactions Assemblages (BIA), BP 71627, 44316 Nantes Cedex 3, France

1 Introduction

Calcium phosphate (CaP) ceramics are the main raw materials used to elaborate granules for bone substitutes. These ceramics are being increasingly used in orthopedic [1] and dental fields [2] because of their bioactive properties. The first injectable polymer-CaP granule composite was introduced by Klein et al. [3]. The concept of injectable calcium phosphate ceramics suspension (ICPCS) developed in our laboratory is based on association of biphasic calcium phosphate (BCP) particles and polysaccharide solution. ICPCS requires suitable rheological properties to ensure bonding of the mineral phase in situ with good cell permeability.

The BCP mineral phase is an association of hydroxyapatite (HA) and β-tricalcium phosphate (β-TCP). The suitable weight proportions of HA (60%) and β-TCP (40%) have provided BCP ceramics with controlled

bioactivity and biocompatibility. The viscous phase of ICPCS is a hydroxypropylmethylcellulose (HPMC) solution, a biocompatible and nontoxic polysaccharide [4]. A similar concept was developed by Chazono et al. [5] using β-TCP granules as the bioactive fillers and sodium hyaluronate (Na-Hyal) as the carrier matrix. Another way of making an injectable calcium phosphate suspension is to use natural anorganic bovine-derived hydroxyapatite matrix (ABM). This is a combination of ABM with a synthetic cell-binding peptide on its surface as the bioactive fillers and the viscous phase is a water solution of glycerol and an ionic cellulosic ether (sodium carboxymethylcellulose) [6].

Rheological properties of ICPCS are based on different parameters (polymer concentration, particles size and volume fraction). In practice, to show better injectability and avoid demixing phenomena and filter pressing of suspension during injection from the syringe, BCP particles must be stable in the suspending medium. The formulation of this type of biomaterial is also an essential factor for its stability during storage. Once a homogenous suspension of solid micron-sized particles with a density higher than that of the suspending fluid is placed inside a container, the particles settle out as a consequence of gravitational force. This physical phenomenon, sedimentation, is observed in various engineering fields such as chemical engineering [7], materials [8], food industry [9] and pharmaceuticals processing [10].

Sedimentation describes the motion of molecules in solutions or particles in suspensions in response to an external force such as gravity. In 1952, Kynch [11] proposed a classical model of sedimentation by introducing the particle flux of a number of particles moving downward per unit of area per unit of time. However, Kynch's theory of sedimentation does not apply to the compression region [12], where the particles accumulate and become concentrated. The excluded volume due to the multi-particle collective interactions in the compressed zone becomes important and needs to be incorporated into the model. Later, Davis and Russel [12] proposed an extension of Kynch's batch sedimentation theory that introduced a diffusion term relating to the osmotic pressure.

Different approaches have been proposed to describe the settling process. In most of the existing models for sedimentation, the concentration and geometrical aspects of the solid particles have been considered, but the role of characteristics of suspending medium has essentially be regarded in terms of its viscosity, rather than its nature [7]. For polymer-based composite biomaterials, analysis of the sedimentation process becomes much more complicated, since the polymer can interact with the particles and eventually promote particle aggregation [7].

To date most publications on modeling of sedimentation have accounted for the effect of particle's nature such as shape, size and density as well as interparticles interactions in concentrated suspensions [7, 8, 13–15]. Among them, several studies have been devoted to the understanding of the stability of suspensions or settling phenomena from a fundamental point of view [13]. With this respect, the most important parameter appears to be the volume fraction of particles, that governs their interactions.

The ICPCS show sedimentation phenomena during storage and it is difficult to shake this product (viscous paste) before use. Therefore, it is better to control the sedimentation. The present study concerns the settling properties of biphasic calcium phosphate particles, at a fixed volume fraction, under different conditions (suspending medium concentration, particle size and sterilization). Our work is dedicated to the understanding of the effect of the formulation on the stability of calcium phosphate suspension before and after steam sterilization, since this step is unavoidable from an applicative point of view. The irradiation of polymeric materials with gamma rays leads to the formation of very reactive intermediates, free radicals, ions and excited states [16, 17]. It was found that hydroxyl radicals (OH) are the main active species for chain breakage of cellulosic polymer molecules [16]. HPMC, as a cellulosic derivative, does not support this sterilization mode [18]. For that, in the present work we used steam sterilization as alternative. By steam sterilization, the polymer does not degrade and the product remains intact without any chemical changes [19].

In a preliminary study [20], the effects of different suspending media and especially different particle sizes were investigated. The role of characteristics of suspending media such as viscosity on the settling of particles was briefly presented, as well as the effect of the polymer molecular weight. The characteristics of the suspending media are here more quantitatively considered and completed by an investigation of the steam sterilization effect. The relevance of this study is that the stability of this suspension is not so easy to reach and we have to know the law of sedimentation before and after the regular steam sterilization process to understand and adapt the formulation of the blend to allow a ready to use injectable biomaterial.

In this paper, we first study the rheological behavior of hydroxypropylmethylcellulose solutions, which will serve as suspending medium of the particles. Secondly, we discuss the stability of calcium phosphate suspensions. The sedimentation study of BCP particles at fixed volume fraction is presented as a function of the viscosity of the suspending medium and the particle size, before and after steam sterilization.

2 Materials and methods

2.1 Materials

2.1.1 BCP particles

The CaP ceramics used in this study was BCP (60% HA and 40% β-TCP) prepared in our laboratory by precipitation of calcium-deficient apatite (CDA) and sintering [21]. The Ca/P ratio of the BCP is 1.6. After sintering at 1050°C during 7 h, the BCP granules were milled and sieved to two ranges (40–80 and 80–200 μm in diameter).

2.1.2 HPMC solutions

The polysaccharide used in this study was HPMC Methocel™ E4M (Colorcon®, UK). As specified by the producer the methoxyl degree of substitution (DS) is 1.9, the methoxyl content is between 28 and 30%, and the hydroxyl content is between 7 and 12%. The average molecular weight is 290,000 Da. Aqueous solutions of HPMC polymer were prepared with deionized water at different concentrations (2 and 3% w/w).

2.2 Methods

2.2.1 SEM analysis

Image observations and granulometry analysis of BCP particles were carried out using scanning electron microscopy (SEM) (LEO 1450 VP, Oberkochen-Zeiss, Germany). Metallization of BCP particles was realized by using a Desk III gold–palladium sputter coater (Denton Vacuum, France). The particle size distribution was determined from high resolution SEM images for a population of over 13000 and 3400 particles (40–80 and 80–200 μm, respectively). Each experiment was performed in triplicates.

Image observations of sediments of ICPCS were realized using SEM. Sediment samples obtained after one week of storage were frozen at −80°C during 24 h and dried. Samples were then sputter-coated with gold–palladium.

2.2.2 Density measurements of BCP particles

The true density of BCP particles was measured using helium pycnometry Micrometrics® AccuPyc 1330 (Bedfordshire, UK). The true density was determined for 660.2 and 650.1 mg of BCP particles (40–80 and 80–200 μm, respectively). Each experiment was performed in triplicates.

2.2.3 Rheological measurements of HPMC solutions

Rheological measurements of HPMC polymer solutions (unsterilized and sterilized samples at 2 and 3% w/w). were carried out at 25°C using the rheometer "RheoStress 300" (ThermoHaake®, Germany) with a titanium cone-plate geometry (60 mm diameter, 1° cone angle, 52 μm gap).

Steady shear tests were carried out to determine flow curves (viscosity vs. shear rate) of polymer solutions. In this study different flow curves could be well describe using the simplified Cross equation [22]:

$$\eta = \frac{\eta_0}{1 + (\lambda\dot{\gamma})^n} \quad (1)$$

where η (Pa s) is the viscosity at a given shear rate $\dot{\gamma}$ (s^{-1}); η_0 (Pa s) is the limiting Newtonian viscosity; λ (s) is the relaxation time and n is the exponent of the power law.

Dynamic oscillatory measurements were carried out to determine storage (G') and loss (G'') moduli of different polymer solutions as a function of frequency (ω) at fixed stress (1 Pa).

Each experiment was performed in triplicates.

2.2.4 Sterilization

HPMC solutions and calcium phosphate suspensions were sterilized by Alphaklave® 23 autoclave (HMCE, France) according to the standard pharmaceutical procedure (121°C during 20 min) [23].

2.2.5 Sedimentation study of BCP particles

Different calcium phosphate suspensions were made by mixing BCP particles (40–80 or 80–200 μm) with HPMC solution (2 or 3% w/w). The blends were mixed with a spatula by addition of BCP particles to HPMC solution. After mixing, the blends were added in the bottle and were sterilized. In the present work, we used a fixed BCP ratio (40% w/w) as published previously [20].

Sedimentation investigations were realized before and after steam sterilization of the suspensions.

The sedimentation study of different suspensions was carried out at room temperature, using 14 mm large and 100 mm height sealed vials. The boundary between the sedimented BCP particles and the clear supernatant phase were determined visually, for each sample, as a function of time (Fig. 1). In parallel, the behavior of the same BCP particles dispersed in deionized water was used as a reference. The volume percentage of the settled BCP particles concentrated phase as a function of time was calculated according to the following formula [20]:

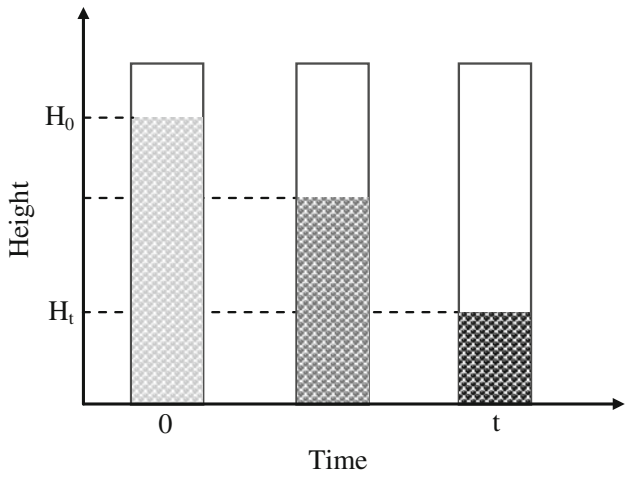

Fig. 1 Schematic representation of settling kinetics. H_t is the height of settled phase at a given time and H_0 is the initial height of the suspension at time 0

$$\text{Height}\,(\%) = \frac{H_t}{H_0} \tag{2}$$

where H_t (m) is the height of settled phase at a given time and H_0 (m) is the initial height of the suspension at time 0. The maximum duration for the sedimentation study was 25 days.

Each experiment was performed in triplicates.

3 Results

3.1 BCP particles

The SEM images (Fig. 2) indicate that the BCP particles are not spherical. Their shape is rather irregular, with sharp edges and does not seem to change drastically with the average size. The particles size distributions (Fig. 3) indicate that distribution clearly displays a maximum for each granulometry. The mean diameters in volume were 70 ± 5 and 170 ± 10 μm for 40–80 μm and 80–200 μm granulometry, respectively.

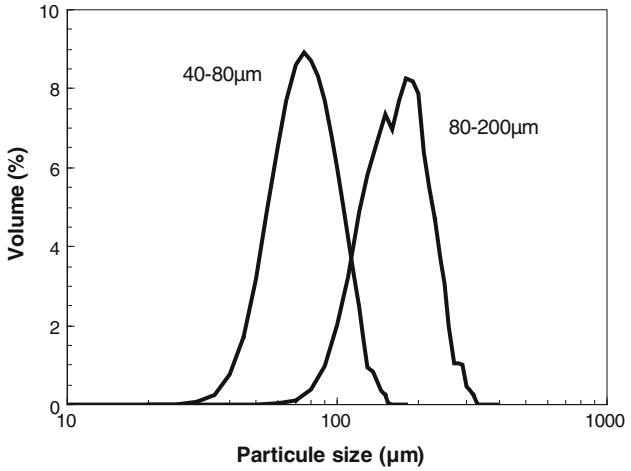

Fig. 3 Particles size volume distributions of BCP. Data obtained from high resolution SEM images for a population of over 13000 and 3400 particles (40–80 and 80–200 μm respectively)

The obtained true density of BCP particles was 3.14 ± 0.02 g cm^{-3} for the both granulometries. This value is still more or less as the estimated value (3.12 g cm^{-3}) obtained from the theoretical density of HA (3.16 g cm^{-3}) [24] and β-TCP (3.07 g cm^{-3}) [25].

3.2 HPMC solutions

3.2.1 Flow curves of HPMC solutions

The flow curves of HPMC solutions are shown in Fig. 4. The steady state viscosities as a function of shear rate were obtained before and after steam sterilization. The flow curves had a similar profile. They all showed a Newtonian zone at low shear rates but at high shear rate they exhibited a shear-thinning behavior. The critical shear rate corresponding to the transition from Newtonian to power law behavior moves to lower values with increasing concentration as found usually for HPMC solutions [4].

The relaxation time (λ), the limiting Newtonian viscosities (η_0) and the exponent of the power law (n) were determined at different concentrations and the values are

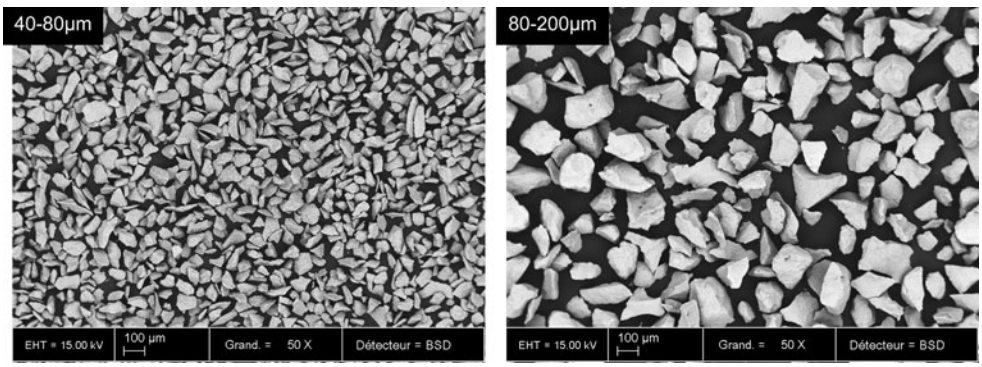

Fig. 2 SEM micrographs of BCP particles (40–80 and 80–200 μm)

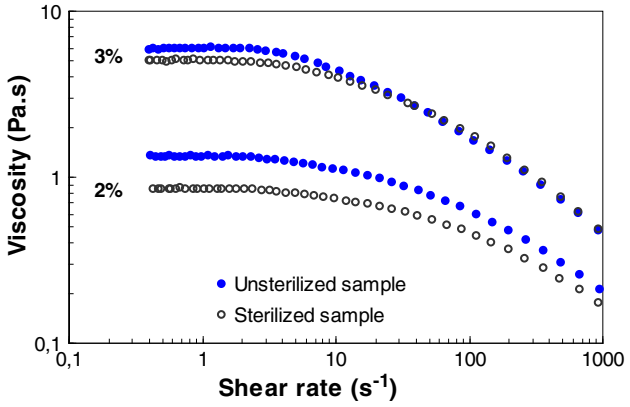

Fig. 4 Flow curves of different HPMC solutions (2 and 3%) at 25°C before and after steam sterilization. Measurements were carried out using a titanium cone-plate geometry (60 mm diameter, 1° cone angle, 52 μm gap)

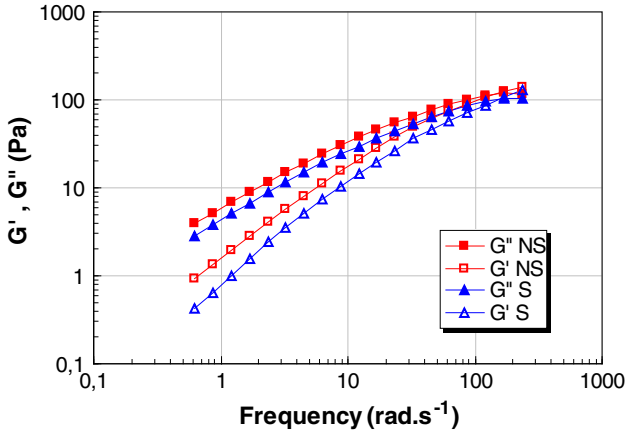

Fig. 5 Storage (G') and loss (G'') moduli dependence on frequency (ω) for HPMC solution (3%) at 25°C before (NS) and after (S) steam sterilization. Measurements were carried out at fixed stress (1 Pa) using a titanium cone-plate geometry (60 mm diameter, 1° cone angle, 52 μm gap)

reported in Table 1. The increase of λ and η_0 with the polymer concentration is usual for entangled polymer solutions as well as the slight decease of the exponent n.

3.2.2 Viscoelastic properties of HPMC solutions

The dynamic storage (G') and loss (G'') moduli of the HPMC solutions were measured. Figure 5 shows mechanical spectra of HPMC solution at 3%. G' and G'' increase strongly with frequency. HPMC solution shows a predominant viscous character at low frequencies, the loss modulus being higher than the storage modulus. The separation between G' and G'' values tends to decrease with an increase of frequency until the cross-over frequency, as it is commonly observed for HPMC solutions [4, 26] as well as water soluble cellulose ethers derivatives [27]. A similar behavior was observed for the 2% HPMC solution (with a higher cross-over frequency—not shown here).

3.2.3 Effect of steam sterilization on rheological behavior

Inhomogeneous solutions and white precipitate were observed right after steam sterilization. Clear solutions were progressively recovered at room temperature (Fig. 6). The limiting Newtonian viscosity, the relaxation time and the exponent of the power law after steam sterilization were characterized (Table 1). For HPMC at 3%, a small difference was remarked on these parameters. A stronger decrease of λ and η_0 after steam sterilization was observed for HPMC at 2%.

Dynamic measurements confirmed the results obtained from flow curves. A small decrease of the dynamic moduli (i.e. G' and G'') before and after steam sterilization of HPMC at 3% was also observed (Fig. 5).

3.3 Sedimentation study of BCP particles

In this section we first describe the settling behavior of calcium phosphate suspensions, as a function of the BCP granulometry and HPMC concentration at a constant BCP ratio. The second part deals with the effect of the steam sterilization.

Densities of the fluids and solid particles; as well as the dimensions of the sieved fillers are given in Table 2. Sedimentation of particles sets in after a given time resulting in the formation of a clear aqueous phase at the top of the tube and sediment phase at the bottom. As the aqueous supernatant phase is perfectly clear, the corresponding profile shows a very sharp and pronounced boundary between the two phases. This boundary moves downward with time. The kinetics of sedimentation were

Table 1 Rheological parameters of HPMC solutions obtained by Cross model

Concentration (% w/w)	Sterilization	Limiting viscosity (Pa s)	Relaxation time (10^{-3} s)	Exponent of the power law
2	Unsterilized	1.50 ± 0.14	14.0 ± 4.88	0.76 ± 0.03
3	Unsterilized	5.59 ± 0.96	28.3 ± 3.47	0.81 ± 0.08
2	Sterilized	0.88 ± 0.02	6.80 ± 1.09	0.78 ± 0.08
3	Sterilized	5.40 ± 0.47	21.7 ± 1.18	0.85 ± 0.07

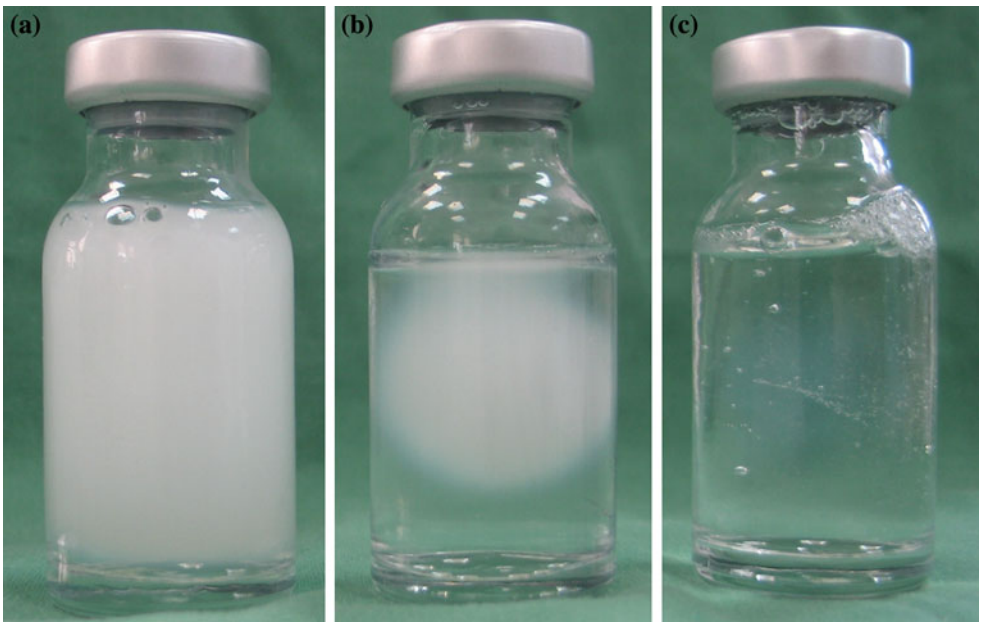

Fig. 6 Photographs of different HPMC solutions at 3%: **a** just after steam sterilization, **b** 1 h after steam sterilization and **c** 1 day after steam sterilization

Table 2 Properties of HPMC solutions and BCP particles used in this study

Material	Size distribution (μm)	Average diameter[a] (μm)	Concentration (% w/w)	Limiting viscosity (Pa s)	Density (g cm^{-3})
HPMC	–	–	2	1.50 ± 0.14	1.10 ± 0.14
HPMC	–	–	3	5.59 ± 0.96	1.22 ± 0.27
BCP	40–80	70 ± 5	–	–	3.14 ± 0.02
BCP	80–200	170 ± 10	–	–	3.14 ± 0.02

[a] Obtained from particles size volume distributions of BCP

obtained very easily by marking visually the sediment volume as a function time.

The data obtained for different HPMC concentrations, BCP granulometries and sterilization effect are displayed in Fig. 7. It can first be seen that the settling is much slower than in pure water and that the level of the sediment is substantially higher. All the curves present, in the beginning of the experiment, a linear section corresponding to a constant sedimentation velocity. After the linear part the settling velocity slows down progressively. The front volume stabilizes at some equilibrium value. The same behavior was observed for sterilized and unsterilized samples. Suspensions with water, as a suspending fluid, showed a very rapid kinetic of sedimentation with a maximal compactness [20].

The influence of the BCP granulometry, HPMC concentration and sterilization effect on the sedimentation properties is quantified in Table 3, where the experimental sedimentation velocity has been reported. Results show clearly that sedimentation velocity (experimental velocity) increases with increasing BCP particle's size and decreasing HPMC concentration. This can readily be expected since both the viscosity and the size of the particles control the sedimentation rate. It is also found that the larger the particles, the larger the sediment volume (although the same volume fraction of particles is present in each case). The sediment volume is also increased, for a given particle size, when the polymer concentration increases.

Assuming that the sedimentation of BCP particles in a gravitational field follows the Stokes law, knowing the particle size, densities and viscosities (Table 2), the Stokes sedimentation velocity can be estimated using Eq. 3 [28]:

$$U_s = \frac{2g(\rho_s - \rho_f)d^2}{9\eta_0} \tag{3}$$

where U_s (m s^{-1}) is the Stokes sedimentation velocity, ρ_s (kg m^{-3}) is the solid-phase density, ρ_f (kg m^{-3}) is the fluid density, d (m) is the sedimentation diameter of a solid-phase particle, g (m s^{-2}) is the gravitational acceleration, and η_0 (Pa s) is the Newtonian viscosity of the suspending fluid. The geometry of particles plays an important role in

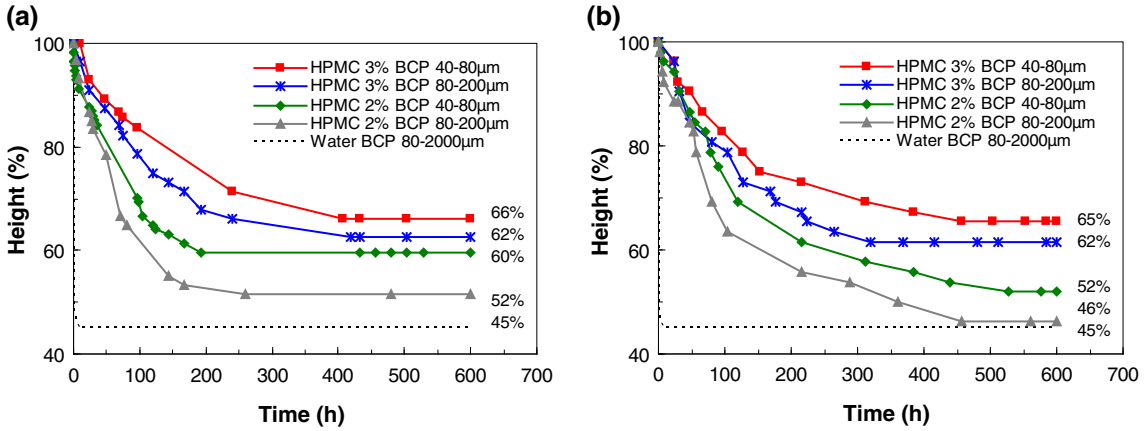

Fig. 7 Settling kinetic for different BCP particles (40–80 and 80–200 µm) with different HPMC concentrations (2 and 3%): **a** unsterilized samples and **b** sterilized samples

sedimentation phenomena. In the Stokes law, particles are considered spherical. So, in the calculation we considered an equivalent diameter for angular particles.

The Stokes equation is applicable only if the Reynolds number (Re) is less than 2 for the lamellar flow region [14]. Reynolds number is given by:

$$Re = \frac{\rho_f U_s d}{\eta_0} \tag{4}$$

where U_s (m s^{-1}) is the Stokes sedimentation velocity, ρ_f (kg m^{-3}) is the fluid density, d (m) is the sedimentation diameter of a solid-phase particle and η_0 (Pa s) is the Newtonian viscosity of the suspending fluid.

Reynolds number can be estimated, from the suspensions characteristics to be in the range, $1.4 \times 10^{-5} < Re < 2.7 \times 10^{-3}$, so that the particles under study were indeed in the Stokes sedimentation region.

Table 3 compares the calculated Stokes velocity of the BCP particles using Eq. 3 (where the mean diameter of the particles has been used) with the experimental velocity. From the experimental data, the experimental velocity of sedimentation in the homogeneous part of the suspension is derived by considering the variation with initial time of the total volume of particles located above a given fixed horizontal plane.

It can be seen that the values of the experimental velocity do not agree with those obtained with Stokes calculation. However, the dependence of the theoretical velocity on particle size and solution concentration was qualitatively obtained. The experimental sedimentation viscosities are systematically lower than the calculated ones. The difference varies between a factor 3 and a factor 70. The largest discrepancies are observed for the largest particles in the 2% solution, whether the suspension has been sterilized or not. This point will be further addressed in the discussion.

At equilibrium, after settling was completed, the boundary between the sedimented BCP particles and the clear supernatant phase remains constant. This value depends on BCP granulometry and HPMC concentration. The final

Table 3 Values of sedimentation velocity and sediment volume obtained for different suspensions

HPMC concentration (% w/w)	BCP size distribution (µm)	Sterilization	Experimental velocity U (m s^{-1})	Stokes velocity U_s (m s^{-1})	U/U_s	Sediment volume[a] (%)
2	40–80	Unsterilized	5.77×10^{-7}	3.63×10^{-6}	1.59×10^{-1}	59.65 ± 2.21
3	40–80	Unsterilized	2.93×10^{-7}	9.16×10^{-7}	3.21×10^{-1}	66.07 ± 3.12
2	80–200	Unsterilized	7.34×10^{-7}	2.13×10^{-5}	3.46×10^{-2}	51.67 ± 1.38
3	80–200	Unsterilized	4.13×10^{-7}	5.39×10^{-6}	7.66×10^{-2}	62.50 ± 2.61
2	40–80	Sterilized	6.11×10^{-7}	6.18×10^{-6}	9.89×10^{-2}	51.92 ± 3.09
3	40–80	Sterilized	3.77×10^{-7}	9.49×10^{-7}	3.98×10^{-1}	65.38 ± 2.57
2	80–200	Sterilized	8.81×10^{-7}	3.61×10^{-5}	2.45×10^{-2}	46.15 ± 1.89
3	80–200	Sterilized	4.82×10^{-7}	5.58×10^{-6}	8.64×10^{-2}	61.54 ± 2.06

[a] Volume fraction inside the sediment at equilibrium

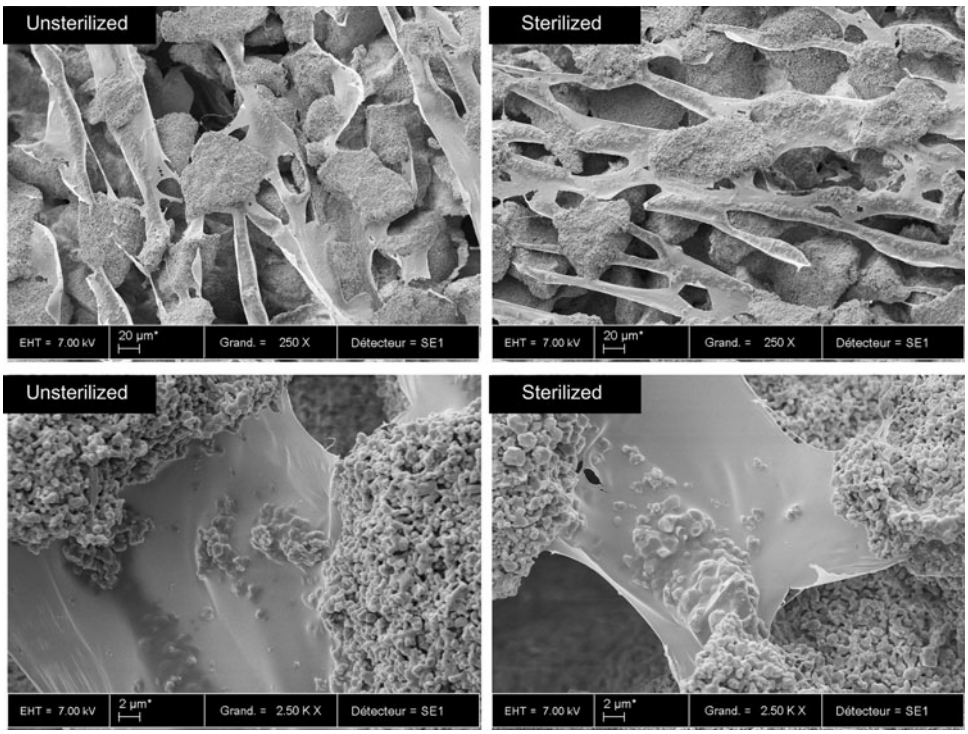

Fig. 8 SEM micrographs of ICPCS sediments after 1 week of storage (BCP ratio = 40% w/w; HPMC concentration = 3%; BCP granulometry = 40–80 µm). Images showing the architectural organization of particles inside the sediment before and after steam sterilization

sediment volume decreases with increasing BCP granulometry and decreasing HPMC concentration (Table 3). The results indicate that the main factor affecting the sediment volume is the polymer concentration and the second one is the particle size.

The settling behavior of each suspension before and after steam sterilization was compared. Results show clearly that the sedimentation velocity increases slightly as it can be expected from a decrease of suspending medium viscosity. The final sediment volume decreases for 2% HPMC solution and is only slightly changed for 3% solution after steam sterilization.

3.4 Morphology of sediments

Figure 8 displays the architectural organization of particles inside the sediment. Both unsterilized and sterilized samples, after one week of storage, show the presence of HPMC on the BCP particles. The HPMC concentration is far above what can be expected from adsorbed chains anchored onto the particles. The measurement of the viscosity of the supernatant solution leads to a remaining polymer concentration of 1.5% for the HPMC solution initially at 2%. The sediment that presents a regular organization of particles and the presentation of the dry polymer observed by SEM were the same before and after steam sterilization. BCP particles (especially of the smallest dimensions) appear imbedded in the polymer layer.

4 Discussion

4.1 Rheology of HPMC solutions

The flow properties of HPMC solutions are typical of those of macromolecular solutions [4]. The limiting Newtonian viscosity (η_0) values obtained at relatively low shear rates increase when the polymer concentration rises, and at the same time the Newtonian plateau limit, as seen by the critical shear rate corresponding to the transition from Newtonian to shear thinning behavior, shifts to a lower shear rates.

The sensitivity of rheological measurement allowed us to evidence changes in the HPMC solution coming from steam sterilization. A decrease after steam sterilization of η_0 and λ was noted for HPMC solution at 2% (w/w). Viscoelastic results confirmed this behavior with a small difference in G' and G'' before and after steam sterilization.

Under the conditions of steam sterilization the different HPMC solutions undergo some gelation followed by the flocculation and formation of aggregates [29, 30]. The heat treatment induced physical gelation of water-soluble polysaccharide solutions as the result of the strong hydrophobic interactions between the polymer chains [31]. The polymer assumed a new spatial configuration after steam sterilization, which appeared to be the main cause of turbidity and phase separation. The decrease in viscosity could be explained by the formation of the irreversible aggregates and considering that rehydration is less favored

than dehydration [32]. The effect of steam sterilization was also studied by Bohic et al. [32]. The light scattering experiments on aqueous solution of HPMC showed that the water affinity is rather good and the results seem to favor chain conformation changes during steam sterilization rather than degradation processes.

Since the intrinsic viscosity measurements (not mentioned in this work) and solely on the basis of the molecular weight before and after steam sterilization, we assume that there is no degradation of HPMC in deionized water. Previously experiments carried out for silted HPMC indicated that macromolecular chains became more "compact" after steam sterilization and the effect was explained by the formation of intra- and intermolecular associations during the sterilization stage originating from the temperature-induced phase separation [33].

4.2 Stability of calcium phosphate suspensions

As already shown above the effect of the particles size on the sedimentation process was obtained. It is found that, at given HPMC concentration, the particles with larger size lead to more rapid settling. As the HPMC concentration is increased, and thus also the viscosity of the suspending medium, the sedimentation rate decreases. If this behavior is in qualitative agreement with the Stokes law, the settling velocity appears always lower than predicted [7, 15, 28]. Furthermore, the divergence with this behavior depends on the concentration and on the size of the particles.

Our experiments have been carried out at a volume fraction of particles (ϕ) of 17.4%, clearly in the semi-dilute or concentrated range. In this regime, collective hydrodynamic interactions have to be taken into account. Different models proposed both empirical [34] and theoretical [35, 36] approaches. Experimental data from the literature were summarized and correlated by several groups [15, 37, 38] in the form of Eq. 5:

$$\frac{U}{U_s} = (1-\phi)^{-K} \tag{5}$$

where U (m s^{-1}) is the experimental sedimentation velocity, U_s (m s^{-1}) is the Stokes sedimentation velocity and K is a negative constant. A value of -6.55 is often considered, so that U/U_s should be on the order of 0.4, in our experimental conditions. Our experimental results (Table 3) lead to the conclusions that even lower sedimentation rates are observed. This effect could be attributed to the presence of a concentrated polymer solution as a suspending medium and to polymer particles interactions. Indeed, the size of the particles is large as compared to the mesh size (ξ) of the polymer solution (estimated at 40 nm for the 3% solution, from the crossing point (G_c) of G' and G'', and assuming that $G_c = \frac{kT}{\xi^3}$, where k is the Boltzmann constant). In addition, polymer chains and BCP particles can interact through (i) adsorbed polymer chains, (ii) interaction between adsorbed chains and free polymer chain in solution and (iii) compression of the polymer network attached or interacting with particles. The coupling between particle aggregation and settling phenomena is responsible for original behaviors as previously reported in the case of calcium carbonate suspensions [13, 39]. Examination of the normalized sedimentation velocity (U/U_s) shows that the largest decrease is observed for the largest particles, which can be understood by the fact that the disturbance they induce on the macromolecular network is higher, and that they are likely to drag a larger amount of polymer into the sediment.

Surprisingly, lowest polymer concentrations lead also to stronger effects, for a reason that is not fully understood. It might be possible that less concentrated polymer solutions lead to increase the backflow effect and thus decrease the sedimentation viscosity.

In order to examine the role of steam sterilization on the stability of calcium phosphate suspensions, the comparison between unsterilized and sterilized suspensions was carried out. It is found that steam sterilization slightly affects the settling behavior of the suspensions. Sedimentation increases after sterilization because HPMC changes its conformation in presence of Ca^{2+} ions [32]. The polymer chains become less hydrophilic and contract its hydrodynamic volume allowing less space between fillers. This can explain the decrease of the sediment volume after steam sterilization. The influence of the parameters (size of the particles and polymer concentration) on the deviation from Stokes law is identical to that of unsterilized solutions.

As far as the sediment is concerned, it has been shown that the sediment volume increases when the polymer concentration increases. This can readily be explained by the fact that polymer chains, not to say part of the polymer solution network are dragged into the sediment. This leads to an increased separation between particles and hence a higher sediment volume. The decrease of the sediment height, when the size of the particles increases, can be explained by a higher consolidation gravitational force with larger particles.

Numerous studies have shown that interconnected macropores are needed to facilitate bone ingrowth [40]. The main advantage of this presentation is the fully interconnected properties [41] of the composite after the matrix dissolution and/or degradation. This experimentation highlights the granules spacer property of hydrophilic macromolecules that is a key issue for interconnection control, one of the better ways to improve osteoconduction and bioactivity. The different HPMC/BCP interactions (polymer-particle and particle–particle) may have an impact on the cohesion of the ceramic particle. This

suggested that particle boundaries did not withstand the pressure initiated from polymer interaction during the settling process or/and during the steam sterilization.

5 Conclusions

An investigation of the settling behavior of calcium phosphate suspension for various conditions has been presented. Studies were realized at fixed BCP ratio as a function of the particle size and suspending medium concentration. The rheological characterization indicates that HPMC polymer could be classified as a macromolecular solution and the influence of steam sterilization on rheological behavior was observed. The heat treatment induced physical gelation of water-soluble polysaccharide solutions as the result from the strong hydrophobic interactions between the polymer chains. The influence of the suspending medium concentration and the particle size on the settling velocity was qualitatively described by Stokes's law. From a quantitative point of view, a strong slowing down of the settling process, as compared to Stokes predictions, has been evidenced, and qualitatively explained in terms of interactions between particles and polymer chains. The investigation of the influence of steam sterilization on the settling kinetics and sediment compactness show a slight difference between unsterilized and sterilized suspensions. The difference between the limiting Newtonian viscosity before and after steam sterilization can account for this observation. To decrease the sedimentation process, the granule size has to be smaller and the polymer concentration has to increase. This experimentation highlights the granules spacer property of hydrophilic macromolecules that is a key issue for interconnection control, one of the better ways to improve osteoconduction and bioactivity.

The limitation of this investigation is due to the application of one type of calcium phosphate suspension. It could be extend to other suspensions.

Acknowledgements This present work was supported by the regional program BIOREGOS (Région Pays de la Loire, France). The help of Paul Pilet (LIOAD INSERM U791, Nantes) for the SEM analysis, Jean-Michel Bouler (LIOAD INSERM U791, Nantes) for BCP preparation, and Stephane Grolleau (CNRS IMN, Nantes) for density measurements is acknowledged with gratitude. We thank Colorcon® for providing the Methocel™ E4M.

References

1. Gauthier O, Bouler JM, Aguado E, Pilet P, Daculsi G. Macroporous biphasic calcium phosphate ceramics: influence of macropore diameter and macroporosity percentage on bone ingrowth. Biomaterials. 1998;19(1–3):133–9.
2. Weiss P, Layrolle P, Clergeau LP, Enckel B, Pilet P, Amouriq Y, et al. The safety and efficacy of an injectable bone substitute in dental sockets demonstrated in a human clinical trial. Biomaterials. 2007;28(22):3295–305.
3. Klein CP, van der Lubbe HB, de Groot K. A plastic composite of alginate with calcium phosphate granulate as implant material: an in vivo study. Biomaterials. 1987;8(4):308–10.
4. Fatimi A, Tassin JF, Quillard S, Axelos MAV, Weiss P. The rheological properties of silated hydroxypropylmethylcellulose tissue engineering matrices. Biomaterials. 2008;29(5):533–43.
5. Chazono M, Tanaka T, Komaki H, Fujii K. Bone formation and bioresorption after implantation of injectable beta-tricalcium phosphate granules–hyaluronate complex in rabbit bone defects. J Biomed Mater Res Part A. 2004;70A(4):542–9.
6. Barros RR, Novaes AB Jr, Roriz VM, Oliveira RR, Grisi MF, Souza SL, et al. Anorganic bovine matrix/p-15 "flow" in the treatment of periodontal defects: case series with 12 months of follow-up. J Periodontol. 2006;77(7):1280–7.
7. Shojaei A, Arefinia R. Analysis of the sedimentation process in reactive polymeric suspensions. Chem Eng Sci. 2006;61(23):7565–78.
8. Balastre M, Argillier JF, Allain C, Foissy A. Role of polyelectrolyte dispersant in the settling behaviour of barium sulphate suspension. Colloids Surf A Physicochem Eng Asp. 2002;211(2–3):145–56.
9. Novales B, Papineau P, Sire A, Axelos MAV. Characterization of emulsions and suspensions by video image analysis. Colloids Surf A Physicochem Eng Asp. 2003;221(1–3):81–9.
10. Gallardo V, Morales ME, Ruiz MA, Delgado AV. An experimental investigation of the stability of ethylcellulose latex: correlation between zeta potential and sedimentation. Eur J Pharm Sci. 2005;26(2):170–5.
11. Kynch GJ. A theory of sedimentation. Trans Faraday Soc. 1952;48:166–76.
12. Davis KE, Russel WB. An asymptotic description of transient settling and ultrafiltration of colloidal dispersions. Phys Fluids A: Fluid Dyn. 1989;1(1):82–100.
13. Allain C, Cloitre M, Wafra M. Aggregation and sedimentation in colloidal suspensions. Phys Rev Lett. 1995;74(8):1478–81.
14. Chen JF, Luo Y, Xu JH, Chen QM, Guo J. Visualization study on sedimentation of micron iron oxide particles. J Colloid Interface Sci. 2006;301(2):549–53.
15. Vesaratchanon JS, Nikolov A, Wasan DT. Sedimentation of concentrated monodisperse colloidal suspensions: role of collective particle interaction forces. J Colloid Interface Sci. 2008;322(1):180–9.
16. Leonhardt J, Arnold G, Baer M, Langguth H, Gey M, Hubert S. Radiation degradation of cellulose. Radiat Phys chem. 1985;25(4–6):899–904.
17. Park PJ, Je JY, Kim SK. Free radical scavenging activity of chitooligosaccharides by electron spin resonance spectrometry. J Agric Food Chem. 2003;51(16):4624–7.
18. Pekel N, Yoshii F, Kume T, Güven O. Radiation crosslinking of biodegradable hydroxypropylmethylcellulose. Carbohydr Polym. 2004;55(2):139–47.
19. Bourges X, Schmitt M, Amouriq Y, Daculsi G, Legeay G, Weiss P. Interaction between hydroxypropyl methylcellulose and biphasic calcium phosphate after steam sterilisation: capillary gas chromatography studies. J Biomater Sci Polym Ed. 2001;12(6):573–9.
20. Fatimi A, Tassin JF, Axelos MAV, Weiss P. Sedimentation study of biphasic calcium phosphate particles. Key Eng Mater. 2008;361–363(1):365–8.
21. Bouler JM, LeGeros RZ, Daculsi G. Biphasic calcium phosphates: influence of three synthesis parameters on the HA/beta-TCP ratio. J Biomed Mater Res. 2000;51(4):680–4.

22. Cross MM. Rheology of non-Newtonian fluids: a new flow equation for pseudoplastic systems. J Colloid Sci. 1965;20:417–26.
23. van Doornmalen J, Kopinga K. Review of surface steam sterilization for validation purposes. Am J Infect Control. 2008;36(2):86–92.
24. Roy J, Martyn MT, Tanner KE, Coates PD. Interfacial stick–slip transition in hydroxyapatite filled high density polyethylene composite. Bull Mater Sci. 2006;29(1):85–9.
25. Li X, Ito A, Sogo Y, Wang X, Legeros RZ. Solubility of Mg-containing beta-tricalcium phosphate at 25°C. Acta Biomater. 2009;5(1):508–17.
26. Fatimi A, Axelos MAV, Tassin JF, Weiss P. Rheological characterization of self-hardening hydrogel for tissue engineering applications: gel point determination and viscoelastic properties. Macromol Symp. 2008;266(1):12–6.
27. Clasen C, Kulicke WM. Determination of viscoelastic and rheooptical material functions of water-soluble cellulose derivatives. Prog Polym Sci. 2001;26(9):1839–919.
28. Kryuchkov YN. Modeling of sedimentation processes for calculating the particle size distributions of disperse systems. Theor Found Chem Eng. 2005;39(5):522–8.
29. Sarkar N. Thermal gelation properties of methyl and hydroxypropylmethylcellulose. J Appl Polym Sci. 1979;24:1073–87.
30. Sarkar N. Kinetics of thermal gelation of methylcellulose and hydroxypropylmethylcellulose in aqueous solutions. Carbohydr Polym. 1995;26:195–203.
31. Sarkar N, Walker LC. Hydration-dehydration properties of methylcellulose and hydroxypropylmethylcellulose. Carbohydr Polym. 1995;27:177–85.
32. Bohic S, Weiss P, Roger P, Daculsi G. Light scattering experiments on aqueous solutions of selected cellulose ethers: contribution to the study of polymer–mineral interactions in a new injectable biomaterial. J Mater Sci Mater Med. 2001;12(3):201–5.
33. Fatimi A, Tassin JF, Turczyn R, Axelos MA, Weiss P. Gelation studies of a cellulose-based biohydrogel: the influence of pH, temperature and sterilization. Acta Biomater. 2009;5(9):3423–32.
34. Richardson JF, Zaki WN. Sedimentation and fluidisation. Part 1. Trans Inst Chem Eng. 1954;32:35–53.
35. Brady JF, Durlofsky LJ. The sedimentation rate of disordered suspensions. Phys Fluids. 1988;31(4):717–27.
36. Buscall R, White LR. The consolidation of concentrated suspensions. Part 1. The theory of sedimentation. J Chem Soc Faraday Trans 1. 1987;83:873–91.
37. Al-Naafa MA, Selim MS. Sedimentation of monodisperse and bidisperse hard-sphere colloidal suspensions. AICHE J. 1992;38(10):1618–30.
38. Auzerais FM, Jackson R, Russel WB. The resolution of shocks and the effects of compressible sediments in transient settling. J Fluid Mech. 1988;195:437–62.
39. Allain C, Cloitre M, Parisse F. Settling by cluster deposition in aggregating colloidal suspensions. J Colloid Interface Sci. 1996;178(2):411–6.
40. Daculsi G, Passuti N. Effect of the macroporosity for osseous substitution of calcium phosphate ceramics. Biomaterials. 1990;11:86–7.
41. Weiss P, Obadia L, Magne D, Bourges X, Rau C, Weitkamp T, et al. Synchrotron X-ray microtomography (on a micron scale) provides three-dimensional imaging representation of bone ingrowth in calcium phosphate biomaterials. Biomaterials. 2003;24(25):4591–601.